Calculation of sputtering yield with obliquely incident light-ions (H^+, D^+, T^+,He^+) and its representation by an extended semi-empirical formula

T. Ono[a,*], M. Ono[a], K. Shibata[b], T. Kenmotsu[c], Z. Li[d], T. Kawamura[e]

[a] *Okayama University of Science, 1-1 Ridai-cho, Kita-ku, Okayama 700-0005, Japan*

[b] *People Software Corp., 1-7-2 Achi, Kurashiki-shi, Okayama 710-0055, Japan*

[c] *Doshisha University, 1-3 Tataratotani, Kyotanabe-shi, 610-0394, Japan*

[d] *Inner Mongolia National University for the Nationalities, Tonglia 028043, People's Republic of China*

[e] *National Institute for Fusion Science, 32-6 Oroshi-cho, Toki-shi, Gifu 509-5292, Japan*

Abstract

With a Monte Carlo code ACAT, we have calculated sputtering yield of fifteen fusion-relevant mono-atomic materials (Be, B, C, Al, Si, Ti, Cr, Fe, Co, Ni, Cu, Zr, Mo, W, Re) with obliquely incident light-ions (H^+, D^+, T^+, He^+) at incident energies of 50 eV to 10 keV. An improved formula for dependence of normalized sputtering yield on incident-angle has been fitted to the ACAT data normalized by the normal-incidence data to derive the best-fit values of the three physical variables included in the formula vs. incident energy. We then have found suitable functions of incident energy that fit these values most closely. The average relative difference between the normalized ACAT data and the formula with these functions has been shown to be less than 10 % in most cases and less than 20 % for the rest at the incident energies taken up for all of the combinations of the projectiles and the target materials considered. We have also compared the calculated data and the formula with available normalized experimental ones for given incident energies. The best-fit values of the parameters included in the functions have been tabulated in tables for all of the combinations for use.

Keywords: Sputtering; Erosion; Plasma-material interactions; First wall materials; Fitting formula; Monte-Carlo method; binary collision approximation; computer simulation

*Corresponding author. *E-mail address*: ono@sp.ous.ac.jp

1. Introduction

D^+, T^+ ions will be used as fuel and He^+ ions by-products from the nuclear reactions in ITER [1]. Light ions such as those ions strike obliquely the plasma-facing materials of fusion devices after moving along the magnetic field lines with gyrations which enter the materials. Then, target atoms will be ejected from the surface if they are recoiled by projectiles and transferred energy (normal to the surface) enough to overcome the surface potential barrier of a material. If sputtered atoms enter the core plasma after going through the boundary plasma which is located outside the core plasma, they possibly deteriorate it due to radiation loss and to diluting it [2]. So, the density of impurity ions in the core plasma is needed to be maintained within certain allowed levels. Be, C, and high-*Z* materials are candidates for the plasma-facing materials of the ITER. Thus, information on the sputtering yield of such plasma-facing materials with slantingly incident light-ions with a wide spread of energies is indispensable to understand impurity production and control in fusion devices. However, such information consists of a vast amount of data. Therefore, it is useful to use as a simple semi-empirical formula as possible which can easily provide sputtering yield data at any angle of incidence and incident energy for any combination of hydrogen-isotopic and helium ions and fifteen fusion-relevant mono-atomic materials (Be, B, C, Al, Si, Ti, Cr, Fe, Co, Ni, Cu, Zr, Mo, W, Re).

Light-ion sputtering at small angles of incidence is due mainly to the knock-out of target atoms generated near the surface by ions backscattered from the deeper region of a solid [3-5], while, at oblique angles, the knock-out process of surface atoms triggered directly by incident ions becomes dominant [6,7]. The knock-out process at large angles is divided roughly into direct and indirect ones, where a ‘direct’ one means the direct knock-off of a surface atom by an incoming ion and an ‘indirect’ one the knock-off of a surface atom by an incident ion which is scattered just before by the other target atom near the surface. While only the indirect one works at oblique angles of incidence, the direct one plays a major role as the angle of incidence increases to grazing angles of incidence.

Based on this mechanism, and taking also into account the probability that a projectile can enter the surface of a solid by adding a corresponding factor to a formula proposed by Sigmund [8], Yamamura et al. [6, 9] developed a semi-empirical formula that can fit sputtering yield data with obliquely incident light-ions, normalized by the normal-incidence one. However, the contribution from the direct knock-out process to the sputtering yield was not fully considered in this formula. Later, Yamamura et al. [7] improved above formula by taking into account the process fully. However, the improved formula does not have explicit incident-energy dependence. Recently, it has been extended by Ono et al. [10] by replacing the three physical variables involved in it with appropriate functions of incident energy of ions. They estimated the best-fit values of the parameters included in these functions using sputtering yield calculated with a Monte-Carlo code ACAT [11] for C, Fe and W materials bombarded by obliquely incident D^+ ions in an incident energy region from 50 eV to 10 keV. They also indicated that the extended formula with these functions well reproduces the normalized sputtering yield data in the energy ranges considered.

The present paper is to extend above work (i) by increasing the sort numbers of incident light-ions (H^+, D^+, T^+, He^+) and of fusion-relevant materials, (ii) by examining reproducibility of the extended

formula (hereafter, referred to as formula, shortly) and the ACAT data by comparing them with existing experimental data for normalized sputtering yield of the ion-target combinations treated at certain incident energies in the experiments, and finally (iii) by tabulating, for use, the estimated best-fit values of the parameters of the functions included in the formula in tables for all of the ion-target combinations considered here.

Intermediately high-Z or high-Z target materials are prerequisite to the knock-out process described above so that it may take place effectively in such materials. On the other hand, beryllium, boron, and carbon materials are rather low-Z ones, and, so, it may work less effectively in these materials. However, if only one simple formula is capable of reproducing normalized sputtering yield at oblique angles of incidence even for such low-Z materials, then it would be convenient and useful for practical purposes. Thus, we have added, as a trade-off, these three materials to the target materials concerned here.

2. Extended semi-empirical formula and calculation details

The improved formula [7] proposed to reproduce incident-angle dependence of normalized sputtering yield is expressed by

$$Y(E,\theta)/Y(E,0) = T^{f} \exp\left[-\Sigma(X-1)\right], \tag{1}$$

where $T = (1+A\sin\theta)/\cos\theta$, and $X = 1/\cos\theta$. $Y(\theta, E)$ and $Y(0, E)$ on the left hand side of eq. (1) are sputtering yields at incident angles θ and 0 measured from the surface normal of a target material and at incident energy E of ions. The term $\sin\theta$ included in T reflects the contribution of the direct knock-out process [7, 10]. The factor Σ corresponds to a physical quantity that is proportional to an effective scattering cross-section of the first layer of the target material for an incoming projectile, and the exponential $\exp(-\Sigma)$ represents roughly a penetration probability that the projectile can go through the first layer of the material to sputter target atoms from the outermost layer. The expression X^{f} was a factor proposed by Sigmund [8]. The quantities f, Σ, and A are all free parameters to be determined by adjusting the formula well to experimental or calculated data.

The appropriate functions of incident energy of ions introduced in eq. (1) in place of the quantities f, Σ, and A are as follows [10];

$$f = a_1 \exp\left\{-a_2 (E - E_f)^{a_3}\right\} + a_4, \tag{2}$$

$$\Sigma = b_1 \exp\left\{-b_2 (E - E_\Sigma)^{b_3}\right\} + b_4, \tag{3}$$

$$A = c_1 \{\log(E - E_A)\}^{1/c_2} + c_3, \quad (4)$$

where a_i, b_i (i=1~4), c_j (j=1~3), E_f, E_Σ, and E_A are all free parameters to be determined by the method mentioned below.

As is cited above, to obtain sputtering yield data we have used the Monte-Carlo simulation code ACAT which treats atomic collisions in an amorphous target material to a binary collision approximation. We have simulated an amorphous material by using the so-called cell-model in which a target atom is assumed to be distributed at random in each unit cubic cell with a lattice constant $R_0 = N^{-1/3}$ (N is the number density of the target atoms) and the surface to be randomly rough in a depth of half a monolayer. We have used Kr-C potential [12] as an inter-atomic potential to simulate atomic collisions. More detailed descriptions on the inter-atomic potential and the energy loss models employed in the calculations are given in Ref.s [11, 13-15].

Since we are now short of experimental data, published thus far, on incident-angle dependence of sputtering yield of above fusion-relevant materials irradiated by light ions, and since the data, if available, are not systematic, we have referred to calculated data with ACAT. The three parameters involved in eq. (1) have been determined by performing a gradient-search least-squares fit [16] of the formula to the ACAT data for target materials irradiated by light ions. By this method of least squares, the parameters have been incremented simultaneously, with the relative magnitudes adjusted so that the resultant direction of search in parameter space is along the gradient (or direction of maximum variation) of χ^2. Then, the minimum values of χ^2 for several different functions with parameters for each of the three physical parameters determined above have been compared to derive finally the optimum function of incident energy.

3. Results and evaluation of the extended semi-empirical formula

First, we compare normalized sputtering yield by the formula, i.e., eq. (1), with that from the ACAT data for Be, Fe, and W target materials at two or three different values of incident energy in Figs. 1-12. Figs. 5 to 12 show the formula agrees very well with all the values for Fe and W materials bombarded by H^+, D^+, T^+, He^+ ions at incident angles and at incident energies. However, a little differences in the values calculated by the formula and the ACAT data exist at intermediately oblique angles of incidence and only at 10 keV for a Be target material, as displayed in Figs. 1-4. The average relative differences in the values by the formula with the best-fit functions and the ACAT data have been shown to be less than 10 % in most cases and less than 20 % for the rest at incident energies for all of the combinations of the projectiles and the target materials considered here.

Second, we compare normalized sputtering yield given by the formula and the ACAT data with that by experiments [17, 18] done only in the energy range considered here for Be, C, Si, Fe, Ni, Cu, Mo, and W target materials in Figs. 13 to 51. From these figures, we can point out a general trend that normalized sputtering yield by the formula and the ACAT data is a little larger than that by the

experimental data, although there are some exceptions. The tendency can be explained qualitatively as follows: ACAT assumes a flat surface, although it considers randomness of the surface in a one-half of R_0: in contrast, the surfaces of the target materials used in experiments are possibly rough to some degrees in a microscopic scale and are possibly composed partly of numerous smaller surfaces whose outward normal lines point roughly to the direction of incoming ions, resulting in reducing effective angles of incidence: as discussed above, since the direct knock-out process works more effectively as angle of incidence becomes larger, this effect gives rise to weaken the contribution from the process to the sputtering yield: as a result, incident-angle dependence of normalized sputtering yield by ACAT calculations is possibly larger than that by experiments.

In what follows, the other tendencies of normalized sputtering yield calculated from the three origins in question obtained from the comparisons are summarized.

(i) The normalized sputtering yield by the formula, the ACAT data, and the experiments agrees well with each other for Si, Ni, Mo, and W target materials, as shown in Figs. 29 and 30, 33-38, 45-50, and 51.

(ii) The normalized sputtering yield given by the three origins is in close agreement with each other for Be material hit by D^+ ions with 300 eV and 3 keV, and He^+ ions with 3 keV at an incident angle of 50^o, while that by the formula and the ACAT data differs somewhat from the one by the experiment at 80^o, as shown, respectively, in Figs. 13-15.

(iii) For B material, while the yield by the formula and the ACAT data does not agree with that by the experimental data for incidence of 400 eV D^+ ions, it fits each other quite well at 8 keV, as demonstrated in Figs. 16 and 17.

(iv) The symbols used in the following to represent the types of carbon materials are explained in Table 1. For C materials, relative differences in the yield due to the three origins depend strongly on the degree of surface roughness like

(iv-a) the yield by the three origins for C/UCHOPG material hit by 1 keV H^+ ions coincides very well with each other at angles of incidence smaller than 75^o, while that by the formula and the ACAT data differs to some extent from the one by the experimental data at 75^o, as illustrated in Fig. 18,

(iv-b) the yield by the three origins for C/UC pol. material irradiated by D^+ ions with 350 eV, 1 keV, and 2 keV coincides with each other quite well, excep for the case at 350 eV and at 80^o for which some difference in the yield exists, as shown in Figs. 19-21, where the surface roughness existed for the 2 keV case [17],

(iv-c) the yield of C/UC- material hit by 50 eV D^+ ions obtained by the experiment differs largely from that by the formula and the ACAT data, while the former still disagrees to some extent with the latter with 2 keV D^+ ions, as illustrated in Figs. 22 and 23, where the surface was indicated to be rough to a higher degree than that of the C/UC pol. material for the 2 keV case [17], and where chemical erosion was observed to increase the yield with 50 eV D^+ ions and at room temperature [17],

(iv-d) the yield of C/UCI pol. material with 2 keV H^+ ions, by the three origins, fits closely each other, as displayed in Fig. 24, where the surface is pointed out to be rough to some degree [17],

(iv-e) the yield of C/UCI material with 2 keV He^+ ions by the experimental data agrees rather closely

with that due to the rest origins, as figured out in Fig. 25, where the surface roughness existed [17],
(iv-f) the yield of C/POCO material by the experimental data for H^+, D^+, and He^+ ions with 2 keV, does not increase with increasing angle of incidence so highly as that due to the other origins, and, thus, has a large difference from that due to the other origins, as shown in Figs. 26-28, where the surface of the material is indicated to be more rough than that of the C/UC- material irradiated by 2 keV D^+ ions and that of the C/UCI material hit by 2 keV He^+ ions [17].
This result suggests that the amorphous target model with a flat surface employed in the ACAT is not possibly adequate to simulate materials with high degrees of surface roughness.
(v) The yield by the formula and the ACAT data fits rather poorly that by the experimental data for Fe material bombarded by 4 keV H^+ ions, while doing rather good at 8 keV, as figured out in Figs. 31 and 32.
(vi) The yield by the formula and the ACAT data agrees rather well with that by the experimental data for Cu material bombarded by D^+ ions with 100 eV and 300 eV, while doing poorly at 50 eV, 1 keV, and 3 keV, and by He^+ ions at 1 keV, as figured out in Figs. 39-44.
The experimental result [19] using Cu material whose surface was rough shows that sputtering yield does not increase with increasing angle of incidence. This trend supports possibly the results using D^+ ions at 300 eV, 3 keV, and He^+ ions at 1 keV, on condition that the surfaces of the Cu materials used in these experiments were also rough to high degrees.

In Tables 2-5, we list the best-fit values of the parameters involved in the functions representing physical parameters f, Σ, and A used in the improved semi-empirical formula for normalized sputtering yield of fusion–relevant mono-atomic target materials (Be, B, C, Al, Si, Ti, Cr, Fe, Co, Ni, Cu, Zr, Mo, W, Re) irradiated by H^+, D^+, and He^+ ions.

4. Summary

With the Monte Carlo code ACAT which treats atomic collisions in a target material to a binary collision approximation, we have calculated sputtering yield of fifteen fusion-relevant mono-atomic materials (Be, B, C, Al, Si, Ti, Cr, Fe, Co, Ni, Cu, Zr, Mo, W, Re) with obliquely incident light-ions (H^+, D^+, T^+, He^+) with incident energies of 50 eV to 10 keV. By referring to the ACAT data, we have determined the best-fit values of the parameters involved in the three functions of incident energy which had been introduced before into the improved semi-empirical formula for dependence of normalized sputtering yield on incident angle. We have evaluated the extended semi-empirical formula with the values derived from the ACAT data and the available experimental data.

The average relative differences in the values by the extended semi-empirical formula and by the ACAT data have been shown to be less than 10 % in most cases and less than 20 % in the rest cases at incident energies for all of the combinations of the projectiles and the target materials considered here.

From comparison of normalized sputtering yield calculated by the formula and the ACAT data with that by experimental data, the formula and the ACAT data have been shown to give generally a little higher values than those by the experimental data. This tendency has been explained qualitatively by the knock-out process if we assume that the surfaces of the target materials used in the experiments

were rough. However, since sputtering yield of a material with a high degree of surface roughness does not increase with increasing angle of incidence so sharply as that of a material with a flat surface, the yield by the formula and the ACAT data has failed in reproducing that by the experiments using the target materials with enhanced degrees of surface roughness. The other detailed tendencies of normalized sputtering yield by the three origins obtained from the comparisons have been summarized in the following.

(i) The normalized sputtering yield by the formula, the ACAT data, and the experimental data agrees well with each other for Si, Ni, Mo, and W target materials.

(ii) The yield given by the three origins fit well with each other for Be material hit by D^+ ions at an incident angle of 50^o, while that by the formula and the ACAT data differs somewhat from the one by the experiment at 80^o.

(iii) The yield for B material hit by 400 eV D^+ ions given by the formula and the ACAT data does not fit that by the experimental data, while it agrees with each other quite well at 8 keV.

(iv) For C materials, relative differences in the normalized sputtering yield due to the three origins depend strongly on the degree of surface roughness like

(iv-a) the yield by the three origins for C/UCHOPG material hit by 1 keV H^+ ions coincides very well with each other at angles of incidence smaller than 75^o, while that by the formula and the ACAT data differs to some extent from the one by the experimental data at 75^o,

(iv-b) the yield by the three origins for C/UC pol. material irradiated by D^+ ions with 350 eV, 1 keV, and 2 keV coincides with each other quite well, excep for the case at 350 eV and at 80^o for which some difference in the yield exists, where the surface roughness existed for the 2 keV,

(iv-c) the yield of C/UC- material hit by 50 eV D^+ ions obtained by the experiment differs largely from that by the formula and the ACAT data, while the former still disagrees to some extent with the latter with 2 keV D^+ ions, where the surface was indicated to be rough to a higher degree than that of the C/UC pol. material for the 2 keV case, and where chemical erosion was observed to increase the yield with 50 eV D^+ ions and at room temperature,

(iv-d) the yield of C/UCI pol. material with 2 keV H^+ ions, by the three origins, fits closely each other, where the surface is pointed out to be rough to some degree,

(iv-e) the yield of C/UCI material with 2 keV He^+ ions by the experimental data agrees rather closely with that due to the rest origins, where the surface roughness existed,

(iv-f) the yield of C/POCO material by the experimental data for H^+, D^+, and He^+ ions with 2 keV, does not increase with increasing angle of incidence so highly as that due to the other origins, and, thus, has a large difference from that due to the other origins, where the surface of the material was indicated to be more rough than that of the C/UC- material irradiated by 2 keV D^+ ions and that of the C/UCI material hit by 2 keV He^+ ions.

(v) The yield of Cu material bombarded by D^+ ions by the formula and the ACAT data accords rather well with that by the experimental data for 100 eV and 300 eV, while doing poorly for 50 eV, 1 keV, and 3 keV, and by He^+ ions with 1 keV.

Finally, we have listed in the tables the best-fit values of the parameters involved in the functions

representing physical parameters f, Σ, and A used in the semi-empirical formula for normalized sputtering yield of fusion–relevant mono-atomic target materials (Be, B, C, Al, Si, Ti, Cr, Fe, Co, Ni, Cu, Zr, Mo, W, Re) irradiated by H^+, D^+, and He^+ ions.

It is needless to say that sputtering yield for any combination of a projectile and a target material mentioned above, at any incident energy and incident angle, can be calculated by eq. (1), i.e., from the extended semi-empirical formula presented here and a formula for sputtering yield for normal incidence [13].

Acknowledgements

This work has been done under the collaboration research of National Institute for Fusion Science.

It is a pleasure to acknowledge cooperation and discussions with Professors T. Tanabe of Kyushu University, K. Ohya of Tokushima University, and Y. Ueda of Osaka University. This work was partly supported by KAKENHI (19055005).

References

[1] *ITER EDA Documentation Series*, No. 7, IAEA (1996).

[2] P.E. Post, R.V. Jensen, C.B. Tarter, W.H. Grasberger, and W.A. Lokke, At. Data Nucl. Data s **20** 397 (1977) 397.

[3] R. Behrisch, G. Maderlechner, B.M.U. Scherzer, and M.T. Robinson, Appl. Phys. **18** (1981) 391.

[4] U. Littmark and S. Fedder, Nucl. Instr. Mech. **194** (1982) 607.

[5] Y. Yamamura and N. Matsunani, N. Itoh, Radiat. Eff. **71** (1983) 65.

[6] Y. Yamamura, Nucl. Instr. Mech. B**2** (1984) 578.

[7] Y. Yamamura, T. Takiguchi, and Z. Li, Kakuyugokenkyu **66/3 222** (1991) 277 (in Japanese).

[8] P. Sigmund, Phys. Rev. **184** (1969) 383; Phy. Rev. **187** (1969) 768.

[9] Y. Yamamura, Y. Itikawa, and N. Itoh, IPPJ-AM-**26**, Institute of Plasma Physics, Nagoya University, 1983.

[10] T. Ono, K. Shibata, T. Kenmotsu, T. Muramoto, Z. Li, and T. Kawamura, J. Nucl. Mater. **363** (2007) 1266.

[11] Y. Yamamura and Y. Mizuno, IPPJ-AM-40, Institute of Plasma Physics, Nagoya University, 1985.

[12] W.D. Wilson, L.G. Haggmark, and J. Biersack, Phy. Rev. B **15** (1977) 2458.

[13] Y. Yamamura and H. Tawara, At. Data Nucl. Data s **62** (2) (1996) 149.

[14] Y. Yamamura, W. Takeuchi, and T. Kawamura, NIFS-DATA-**45** (1998).

[15] Z. Li, T. Kenmotsu, T. Kawamura, T. Ono, and Y. Yamamura, Nucl. Instr. Methods B **153** (1999) 331.

[16] P.R. Bevington, *Data Reduction and Error Analysis for the Physical Sciences* (MacGraw-Hill, New York 1969).

[17] W. Eckstein, C. Garcia-Rosales, and J. Roth, Max-Planck Institut für Plasmaphysik, Report IPP **9/82**, 1993.

[18] R. Behrisch, W. Eckstein (Eds.), *Sputtering by Particle Bombardment*, Top. Appl. Phy. **110**

(Springer, Berlin, Heidelberg, 2007).
[19] M. Stepanova, S.K. Dew, Phys. Rev. B **66** (2002) 125407.

Table 1 Explanation of the symbols representing types of carbon materials in the text and Figs 18-28.

Symbol	Explanation	Sources
C/UCHOPG	Highly oriented polycrystalline pyrolytic graphite of Union Carbide	[1]
C/UC pol.	Polished pyrolytic graphite of Union Carbide	[2]
C/UC-	Pyrolytic graphite (basal plane) of Union Carbide	[2]
C/UCI pol.	Polished pyrolytic graphite of Union Carbide	[2]
C/UCI	Pyrolytic graphite (edge plane) of Union Carbide	[3]
C/POCO	POCO graphite of POCO Graphite	[2], [3]

Sources:

[1] A.A. Haasz, J.W. Davis, C.H. Wu, J. Nucl. Mater. 162-164 (1989) 915.

[2] J. Roth, W. Eckstein, E. Gauthier, J. Laszlo, Nucl. Mater. 179-181 (1991) 34.

[3] J. Roth, Physical sputtering of solids at ion bombardment, in: Physics of Plasma-Wall Interactions in Controlled Fusion, eds. D.E. Post, R. Behrisch, (Plenum 1986), p. 351.

Table 2 Parameter values of the functions representing coefficients *f*, *Σ*, and *A* for 15 materials hit by H^+ ions.

	$f = a_1 \exp\left\{-a_2\left(E-E_f\right)^{a_3}\right\}+a_4$					$\Sigma = b_1 \exp\left\{-b_2\left(E-E_\Sigma\right)^{b_3}\right\}+b_4$					$A = c_1\left\{\log\left(E-E_A\right)^{1/c_2}\right\}+c_3$			
	a_1	a_2	a_3	a_4	E_f	b_1	b_2	b_3	b_4	E_Σ	c_1	c_2	c_3	E_A
H→Be	12.199	0.58967	0.14396	0.38985	-4084.1	2.1761	0.53331	0.19062	-0.033478	37.076	0.39862	1.7355	-0.20733	28.731
H→B	16.702	0.55021	0.14509	0.13906	-11625	4.108	1.0279	0.13774	-0.014652	48.622	7.8049	14.701	-7.8624	37.084
H→C	16.674	0.54805	0.14537	-0.078509	-8148.9	3.7691	0.93955	0.070533	-0.55217	92.165	5.8739	7.2314	-6.2753	28.959
H→Al	9.821	0.62769	0.13512	0.54859	-4643.9	2.3759	0.60207	0.20371	0.038242	25.511	25.333	18.668	-26.518	-117.05
H→Si	23.005	0.48917	0.14063	-1.3713	-20909	10.794	1.7248	0.11941	0.012374	-40.277	40.259	21.535	-42.014	-196.31
H→Ti	26.002	0.47503	0.14044	-1.5998	-29386	3.8154	1.2645	0.10842	-0.027224	173.32	41.177	22.723	-43.037	-215.61
H→Cr	33.599	0.45745	0.14429	-2.5696	-28109	5.2579	1.3473	0.1023	-0.049357	176.76	40.121	12.045	-44.403	-2120.8
H→Fe	39.204	0.44021	0.1436	-2.9984	-52829	8.8194	1.6412	0.11829	0.050757	147.22	40.958	18.832	-43.515	-949.35
H→Co	41.42	0.43414	0.14321	-3.1513	-67363	12.966	1.6307	0.14236	0.097966	112.09	40.872	15.785	-44.054	-1397.8
H→Ni	43.041	0.43285	0.14394	-3.4167	-61392	14.167	1.6364	0.14398	0.093386	95.419	40.901	14.24	-44.431	-1351.6
H→Cu	41.279	0.43745	0.14426	-3.2956	-55027	7.5065	1.8279	0.094345	0.011584	166.54	42.128	16.193	-45.143	-791.89
H→Zr	-4.7816	0.16688	0.46109	1.6419	-228.96	112.74	1.7448	0.18714	0.097923	-432.79	42.683	16.716	-45.603	-528.72
H→Mo	-12.678	0.14577	0.4738	1.7475	-443.63	110.64	1.5626	0.18918	0.11172	-917.13	40.459	12.455	-44.526	-1442.6
H→W	-8.4803	0.12159	0.4176	1.5823	-802.29	152.6	1.5741	0.19653	0.10612	-687.15	39.003	7.3306	-46.976	-8393.1
H→Re	-7.5226	0.13375	0.45629	1.5386	-1187.8	252.94	1.8365	0.1825	0.10665	-464.76	41.456	9.541	-47.38	-2596.9

Table 3 Parameter values of the functions representing coefficients *f*, *Σ*, and *A* for 15 materials hit by D^+ ions.

	$f = a_1 \exp\left\{-a_2\left(E-E_f\right)^{a_3}\right\}+a_4$					$\Sigma = b_1 \exp\left\{-b_2\left(E-E_\Sigma\right)^{b_3}\right\}+b_4$					$A = c_1\left\{\log\left(E-E_A\right)^{1/c_2}\right\}+c_3$			
	a_1	a_2	a_3	a_4	E_f	b_1	b_2	b_3	b_4	E_Σ	c_1	c_2	c_3	E_A
D→Be	9.9483	0.62236	0.1445	0.57267	-2187.8	1.9491	0.47376	0.1904	-0.067587	32.03	0.20744	1.3005	0.11489	-129.6
D→B	8.3471	0.66681	0.14777	1.012	-1847.5	1.834	0.42808	0.20999	-0.018938	37.731	0.97472	3.3503	-0.7636	7.9452
D→C	6.2783	0.65907	0.13291	0.9646	-1528.8	2.3599	0.59341	0.1905	0.0050363	24.746	7.5142	13.444	-7.567	-33.245
D→Al	3.3272	0.77087	0.17063	1.3567	-2.5291	2.9773	0.84648	0.16794	0.02485	38.035	35.35	30.588	-36.203	-45.482
D→Si	3.0905	1.1262	0.095033	1.2598	-27.013	3.1805	0.8272	0.19221	0.063449	10.16	38.845	34.533	-39.642	-31.679
D→Ti	8.2611	0.51963	0.13383	0.25406	-8382.9	12.465	1.2295	0.19216	0.10727	-36.817	39.497	18.611	-41.821	-737.55
D→Cr	5.911	0.12239	0.43023	1.5157	-1101.4	18.089	1.1729	0.19866	0.12261	-48.181	39.848	23.665	-41.718	-735.92
D→Fe	2.7487	0.10606	0.39251	1.3652	-1714.3	19.339	1.2012	0.20583	0.12424	-62.909	39.08	13.37	-42.713	-1732.1
D→Co	3.5186	0.094713	0.38011	1.2519	-2718.2	11.485	1.2324	0.18053	0.11429	14.584	33.992	10.923	-37.943	-1796.7
D→Ni	2.7384	0.10112	0.38425	1.3648	-1960.5	24.595	1.245	0.20012	0.12159	-110.98	39.709	20.31	-41.963	-983.11
D→Cu	2.7284	0.10506	0.39142	1.3268	-2031.7	12.169	1.4129	0.16289	0.10005	-3.9839	43.375	22.75	-45.45	-619.14
D→Zr	1.2311	0.09136	0.35673	1.329	-3937.5	14.653	1.4397	0.17848	0.09039	41.545	43.534	20.458	-45.816	-372.07
D→Mo	2.2766	0.10645	0.38909	1.4403	-1995.6	33.992	1.3199	0.19962	0.10737	-145.27	43.064	15.484	-46.413	-1137.1
D→W	-3.9199	0.13687	0.42822	1.3886	-622.34	21894	1.1682	0.27326	0.10755	-3709.5	37.271	2.8564	-62.601	-24218
D→Re	-12.233	0.097106	0.45191	1.4951	-3025.4	24613	1.1977	0.27845	0.13215	-2861	41.034	8.4386	-48.071	-5593.4

Table 4 Parameter values of the functions representing coefficients *f*, *Σ*, and *A* for 15 materials hit by T^+ ions.

	$f = a_1 \exp\{-a_2(E-E_f)^{a_3}\} + a_4$					$\Sigma = b_1 \exp\{-b_2(E-E_\Sigma)^{b_3}\} + b_4$					$A = c_1\{\log(E-E_A)^{1/c_2}\} + c_3$			
	a_1	a_2	a_3	a_4	E_f	b_1	b_2	b_3	b_4	E_Σ	c_1	c_2	c_3	E_A
T→Be	7.9467	0.65885	0.14374	0.77933	-1025.4	1.9975	0.42193	0.21805	-0.030483	-8.0622	0.18992	0.94363	-0.12544	-5085.8
T→B	7.0779	0.70948	0.15248	1.2042	-1015.2	1.9512	0.46456	0.19718	-0.038115	30.427	-0.040607	1.3197	0.72293	-177.19
T→C	6.4188	0.71408	0.14931	1.2239	-1103	1.7635	0.43021	0.20772	-0.018208	22.262	7.7342	32.771	-7.3551	-169.76
T→Al	3.477	0.7451	0.19652	1.3606	8.3748	1.7959	0.50098	0.21667	0.035333	35.5	38.487	44.579	-38.96	3.4382
T→Si	2.9844	0.78899	0.081828	0.84167	47.77	1.6013	0.57364	0.18261	0.007159	46.992	40.591	40.674	-41.223	-11.092
T→Ti	8.7484	0.1146	0.43168	1.3756	-1684.9	1.6181	0.48935	0.18537	-0.024994	84.116	40.493	26.358	-41.986	-249.4
T→Cr	9.2206	0.11327	0.43095	1.4364	-1828.4	1.8508	0.41932	0.20943	0.0025335	79.006	41.997	40.26	-43.013	-265.26
T→Fe	9.6651	0.10734	0.424	1.3119	-2431.3	1.7217	0.43125	0.2008	-0.013696	83.017	43.021	22.783	-45.083	-604.78
T→Co	31.84	0.092234	0.4329	1.2274	-6830.8	1.7486	0.49939	0.17631	-0.037206	90.102	43.705	24.458	-45.653	-606.93
T→Ni	9.2645	0.10005	0.41216	1.2677	-3610.9	1.6775	0.44189	0.1974	-0.0081354	87.81	41.885	28.88	-43.401	-423.7
T→Cu	11.33	0.11238	0.43564	1.2662	-2262.7	1.3151	0.38067	0.19884	-0.027365	89.596	41.386	23.561	-43.215	-399.16
T→Zr	17.461	0.090271	0.42444	1.2613	-8415.2	1.1732	0.51611	0.19649	0.041847	173.26	42.534	21.311	-44.619	-288.9
T→Mo	6.0423	0.10783	0.41726	1.3774	-2727.8	1.8118	0.54908	0.20823	0.068839	161.25	43.388	20.918	-45.672	-482.92
T→W	-4.6337	0.14406	0.44579	1.2916	-767.03	21009	1.2819	0.29001	0.12478	-1366	37.279	2.8527	-62.602	-23719
T→Re	-7.2108	0.14616	0.46107	1.3467	-609.62	21752	1.2911	0.29152	0.13573	-1295.6	37.282	2.8558	-62.577	-23879

Table 5 Parameter values of the functions representing coefficients *f*, *Σ*, and *A* for 15 materials hit by He^+ ions.

	$f = a_1 \exp\left\{-a_2\left(E-E_f\right)^{a_3}\right\}+a_4$					$\Sigma = b_1 \exp\left\{-b_2\left(E-E_\Sigma\right)^{b_3}\right\}+b_4$					$A = c_1\left\{\log\left(E-E_A\right)^{1/c_2}\right\}+c_3$			
	a_1	a_2	a_3	a_4	E_f	b_1	b_2	b_3	b_4	E_Σ	c_1	c_2	c_3	E_A
He→Be	7.3798	0.1245	0.4384	1.47	-821.22	4.1142	0.41316	0.27879	0.065038	-219.77	7.8577	205.93	-7.2148	-4635.6
He→B	8.5018	0.10303	0.41235	1.429	-2197.4	5.6778	0.38038	0.27615	0.04402	-875.27	7.8549	187.36	-7.2177	-10226
He→C	9.7382	0.10553	0.42215	1.5102	-2071.4	6.6422	0.37932	0.28097	0.059464	-1106.9	-23.101	2403.6	23.813	86.176
He→Al	6.5317	0.68902	0.24588	1.2503	-33.345	2.0531	0.53761	0.21801	0.054204	28.043	39.325	38.152	-40.025	-32.289
He→Si	2.5141	0.66629	0.1985	1.1921	36.062	1.4964	0.51691	0.19386	0.010214	45.531	39.925	37.781	-40.646	-36.988
He→Ti	2.6432	0.45091	0.13157	0.66646	38.149	3.7357	0.89582	0.17072	0.058489	26.524	41.579	28.572	-42.884	-166.53
He→Cr	12.394	0.11831	0.44574	1.3565	-1228.9	1.956	0.40979	0.2178	0.031695	54.495	41.511	41.549	-42.323	-83.754
He→Fe	12.101	0.11587	0.44124	1.266	-1521.8	1.9693	0.46499	0.20575	0.030578	56.826	45.551	32.049	-46.884	-252.73
He→Co	12.535	0.1125	0.43736	1.2338	-1758.4	2.2517	0.48414	0.21323	0.051137	49.42	44.032	26.188	-45.749	-395.01
He→Ni	13.88	0.10983	0.43581	1.2105	-1967.2	2.625	0.63128	0.17139	-0.0044384	51.835	41.868	22.724	-43.766	-416.85
He→Cu	13.706	0.11943	0.44948	1.1644	-1715.1	2.1465	0.61224	0.18169	0.029341	52.326	42.037	26.931	-43.581	-325.86
He→Zr	9.6724	0.10311	0.41383	1.2317	-3296.1	1.0491	0.33047	0.15267	-0.16905	190.69	44.602	33.84	-45.672	51.832
He→Mo	15.134	0.099872	0.42962	1.2493	-3137.9	1.2065	0.32583	0.17945	-0.1046	181.1	44.062	24.658	-45.828	-158.93
He→W	3.8743	0.084799	0.38056	1.1712	-11968	4.8444	0.55452	0.27838	0.14275	92.124	42.579	12.552	-46.889	-1718.4
He→Re	-8.3106	0.15152	0.47291	1.2608	-670.32	22.231	1.2479	0.21728	0.1566	31.568	42.277	11.465	-47.223	-2982.2

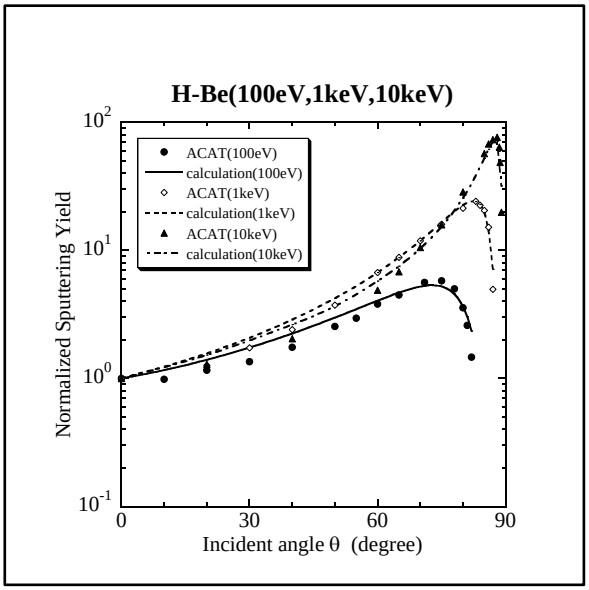

Fig. 1 Normalized sputtering yield vs. incident angle by the formula with the functions and the ACAT data for Be material irradiated by H^+ ions with 100eV, 1keV, and 10keV.

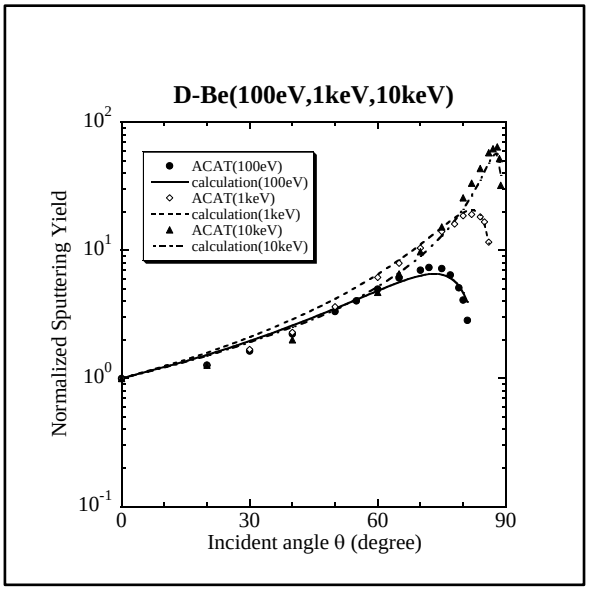

Fig. 2 Normalized sputtering yield vs. incident angle by the formula with the functions and the ACAT data for Be material irradiated by D^+ ions with 100eV, 1keV, and 10keV.

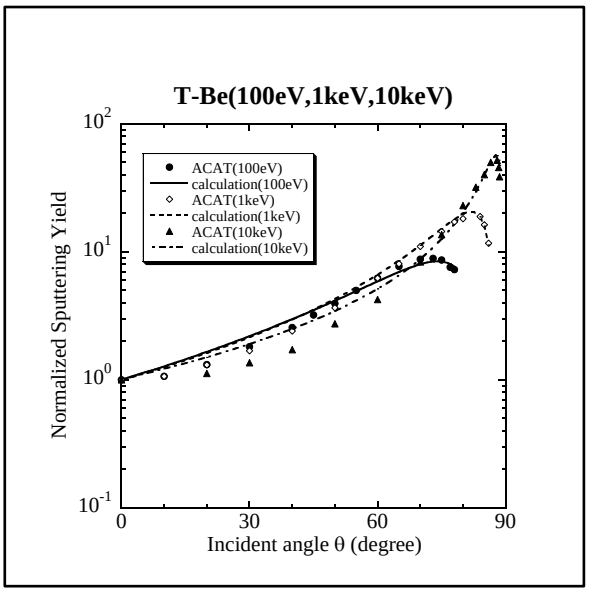

Fig. 3 Normalized sputtering yield vs. incident angle by the formula with the functions and the ACAT data for Be material irradiated by T^+ ions with 100eV, 1keV, and 10keV.

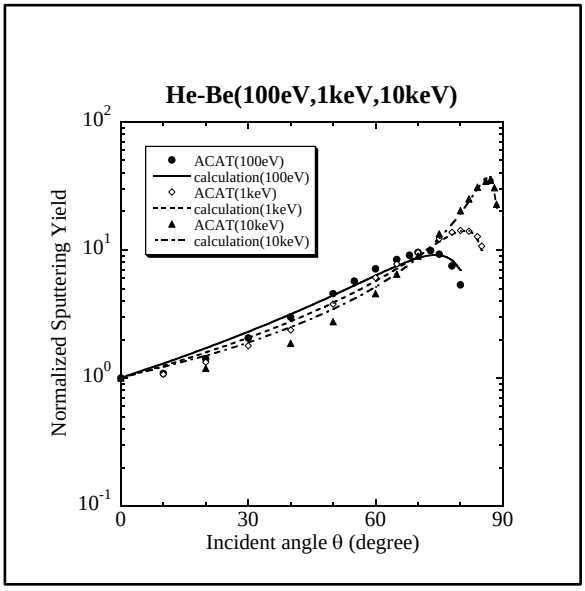

Fig. 4 Normalized sputtering yield vs. incident angle by the formula with the functions and the ACAT data for Be material irradiated He^+ by ions with 100eV, 1keV, and 10keV.

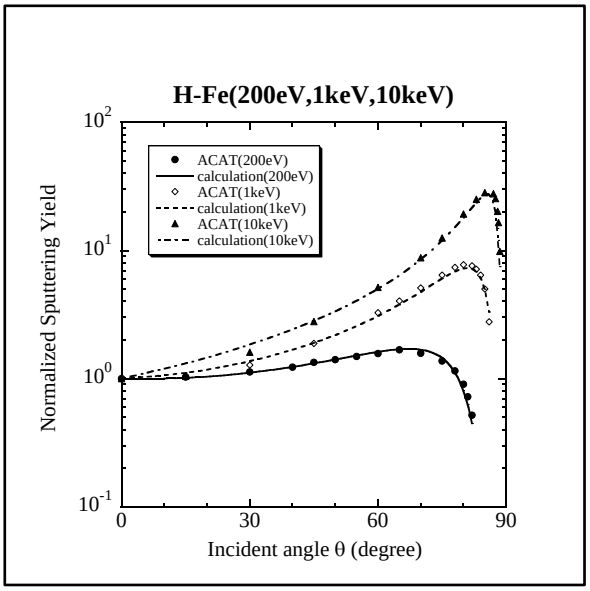

Fig. 5 Normalized sputtering yield vs. incident angle by the formula with the functions and the ACAT data for Fe material irradiated by H^+ ions with 200eV, 1keV, and 10keV.

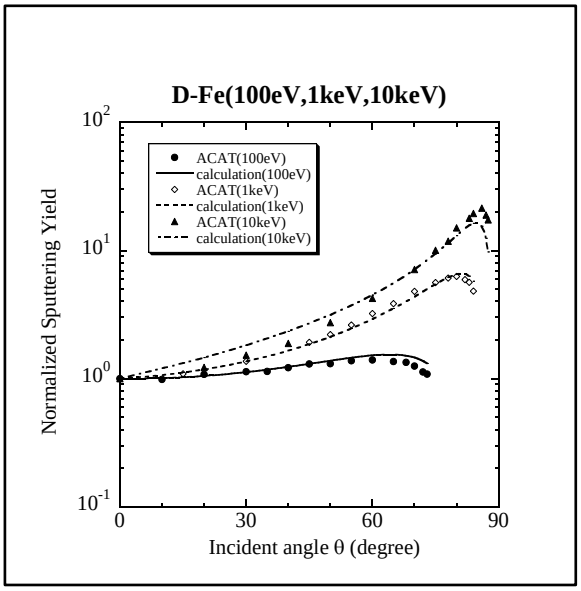

Fig. 6 Normalized sputtering yield vs. incident angle by the formula with the functions and the ACAT data for Fe material irradiated by D^+ ions with 100eV, 1keV, and 10keV.

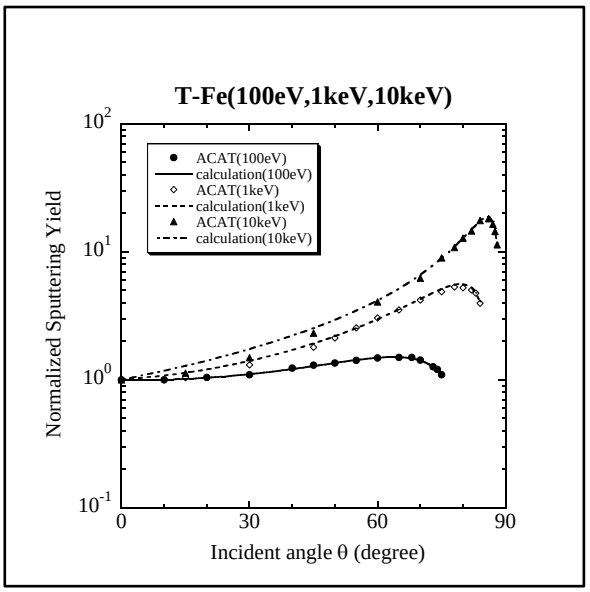

Fig. 7 Normalized sputtering yield vs. incident angle by the formula with the functions and the ACAT data for Fe material irradiated by T^+ ions with 100eV, 1keV, and 10keV.

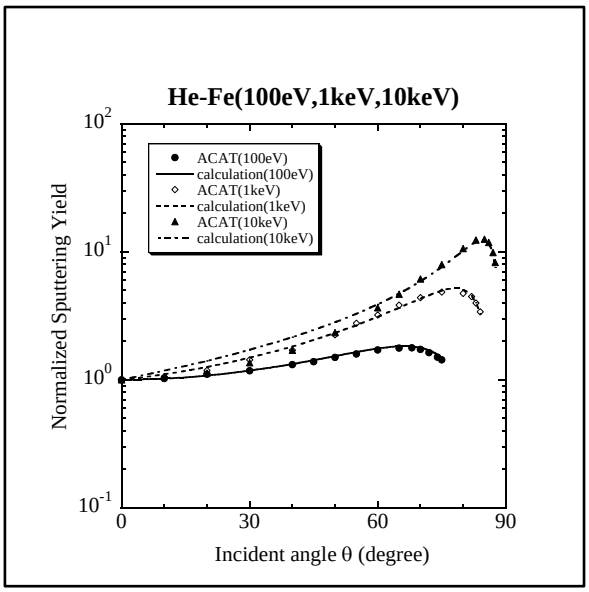

Fig. 8 Normalized sputtering yield vs. incident angle by the formula with the functions and the ACAT data for Fe material irradiated by He^+ ions with 100eV, 1keV, and 10keV.

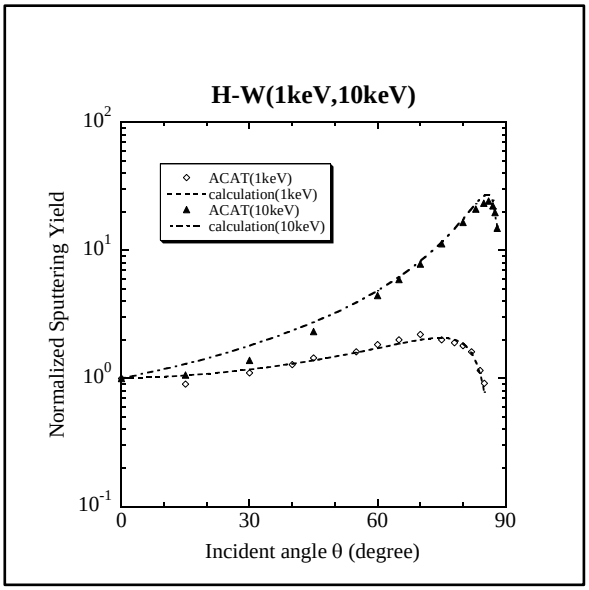

Fig. 9 Normalized sputtering yield vs. incident angle by the formula with the functions and the ACAT data for W material irradiated by H^+ ions with 1keV and 10keV.

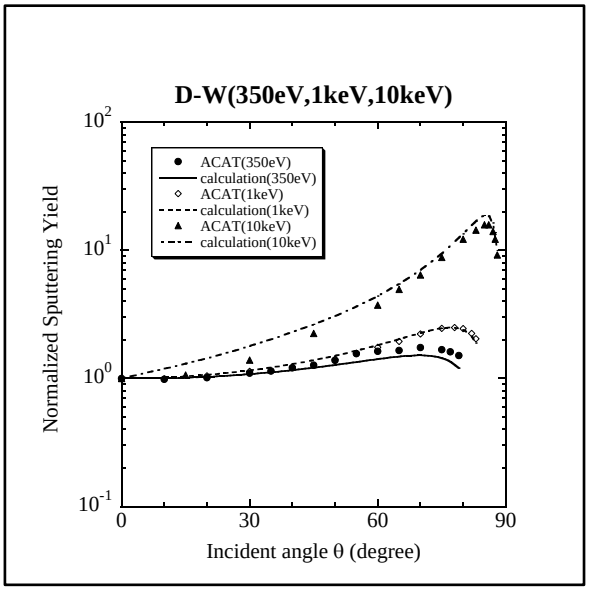

Fig. 10 Normalized sputtering yield vs. incident angle by the formula with the functions and the ACAT data for W material irradiated by D^+ ions with 350eV, 1keV, and 10keV.

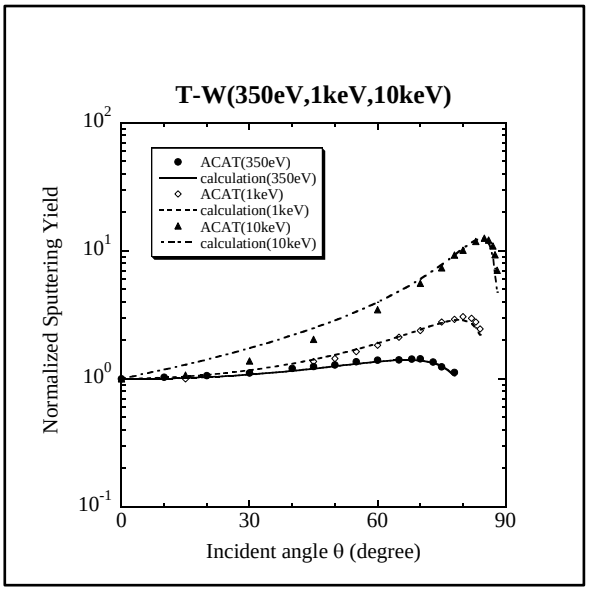

Fig. 11 Normalized sputtering yield vs. incident angle by the formula with the functions and the ACAT data for W material irradiated by T^+ ions with 350 eV, 1keV, and 10keV.

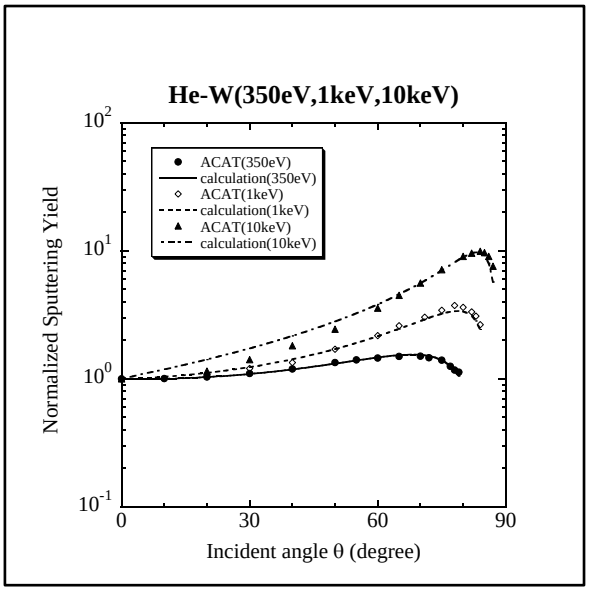

Fig. 12 Normalized sputtering yield vs. incident angle by the formula with the functions and the ACAT data for W material irradiated by He^+ ions with 350 eV, 1keV, and 10keV.

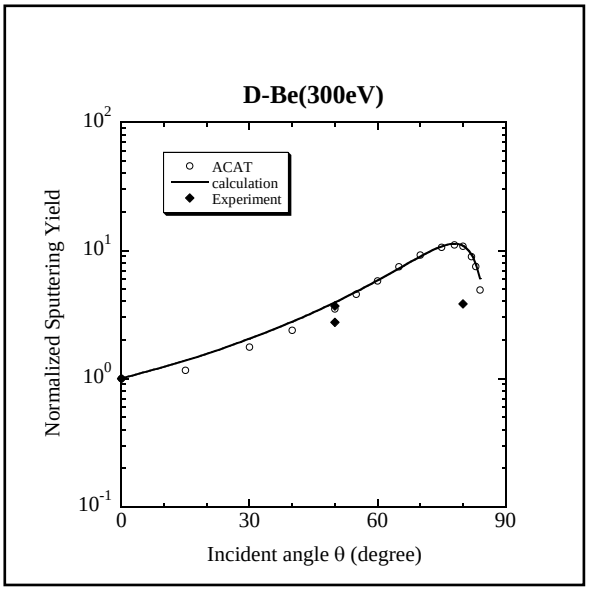

Fig. 13 Normalized sputtering yield vs. incident angle by the formula with the functions, the ACAT data, and the experimental data for Be material irradiated by D^+ ions with 300eV.

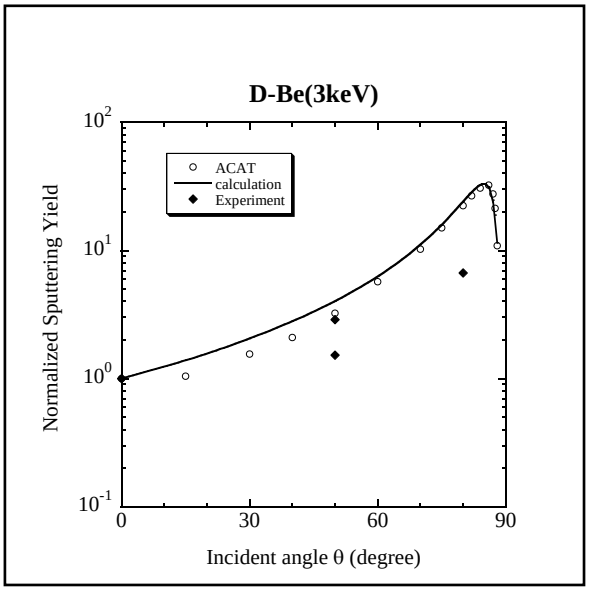

Fig. 14 Normalized sputtering yield vs. incident angle by the formula with the functions, the ACAT data, and the experimental data for Be material irradiated by D^+ ions with 3keV.

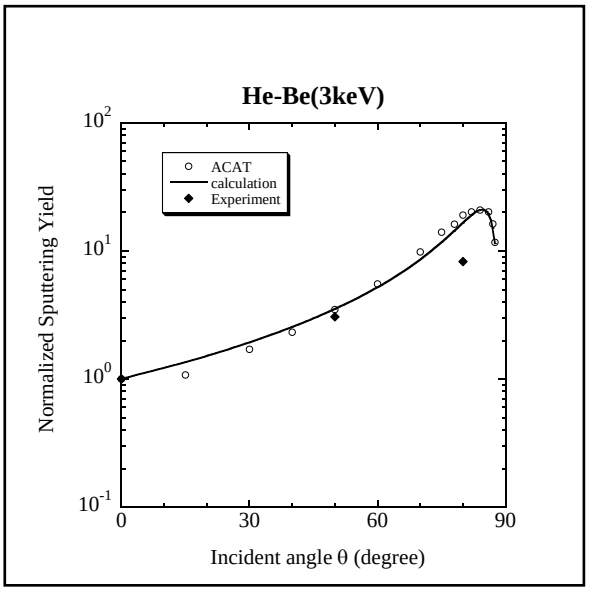

Fig. 15 Normalized sputtering yield vs. incident angle by the formula with the functions, the ACAT data, and the experimental data for Be material irradiated by He^+ ions with 3keV.

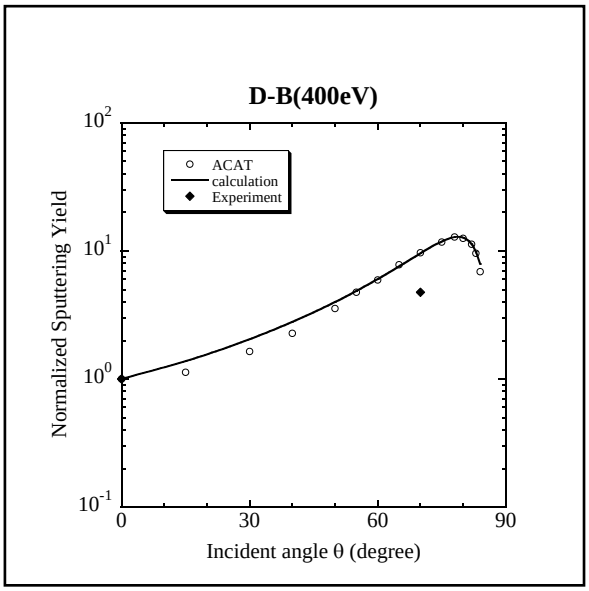

Fig. 16 Normalized sputtering yield vs. incident angle by the formula with the functions, the ACAT data, and the experimental data for B material irradiated by D^+ ions with 400eV.

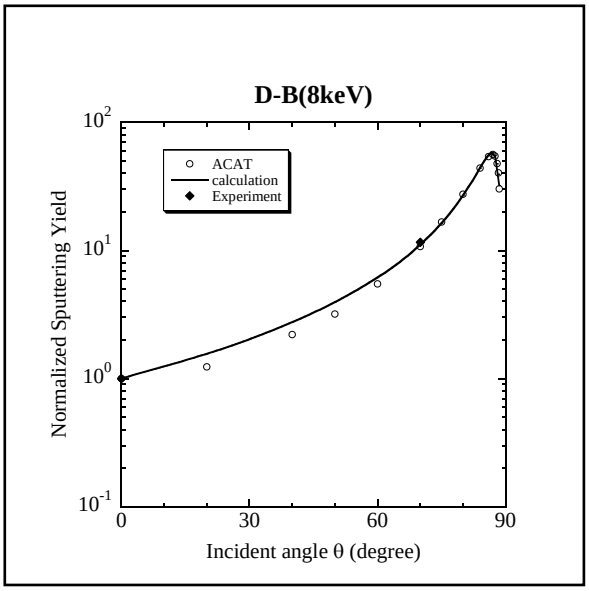

Fig. 17 Normalized sputtering yield vs. incident angle by the formula with the functions, the ACAT data, and the experimental data for B material irradiated by D^+ ions with 8keV.

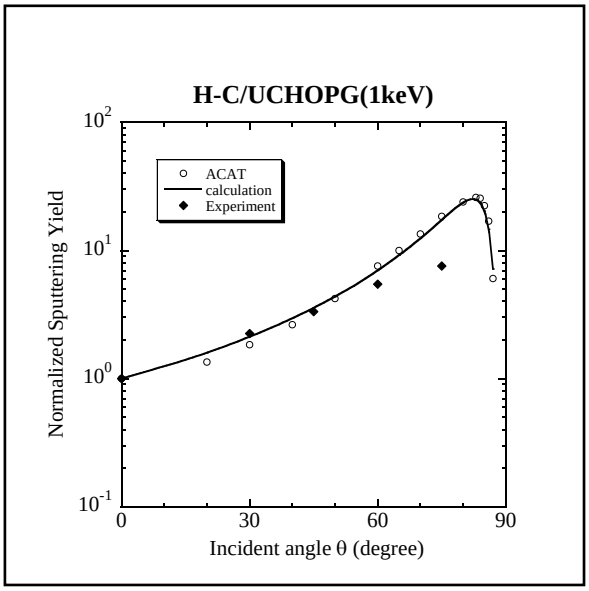

Fig. 18 Normalized sputtering yield vs. incident angle by the formula with the functions, the ACAT data, and the experimental data for C/UCHOPG material irradiated by H^+ ions with 1keV.

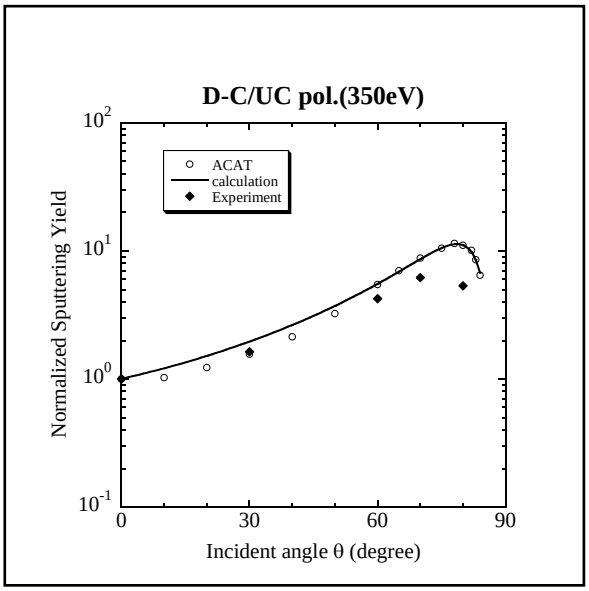

Fig. 19 Normalized sputtering yield vs. incident angle by the formula with the functions, the ACAT data, and the experimental data for C/UC pol. material irradiated by D^+ ions with 350eV.

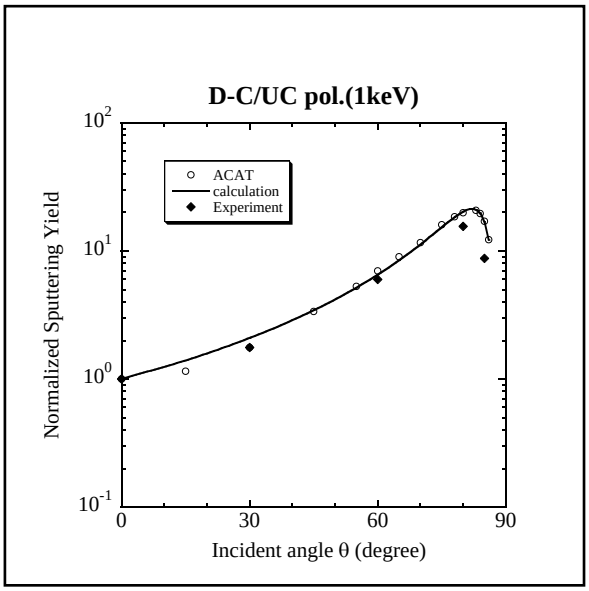

Fig. 20 Normalized sputtering yield vs. incident angle by the formula with the functions, the ACAT data, and the experimental data for C/UC pol. material irradiated by D^+ ions with 1keV.

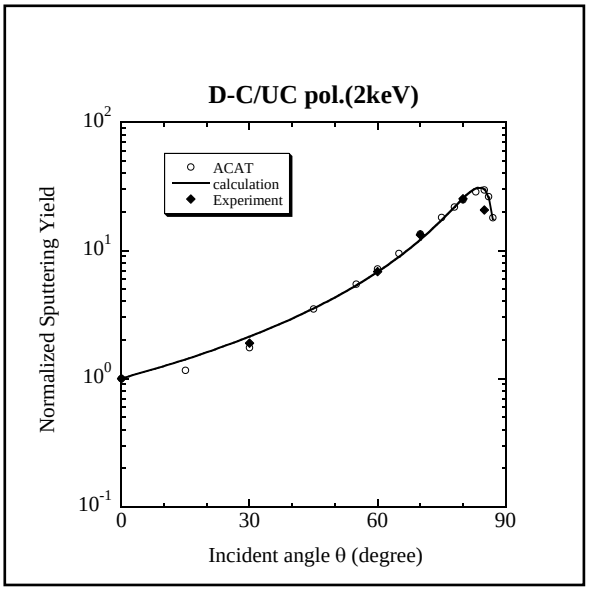

Fig. 21 Normalized sputtering yield vs. incident angle by the formula with the functions, the ACAT data, and the experimental data for C/UC pol. material irradiated by D^+ ions with 2keV.

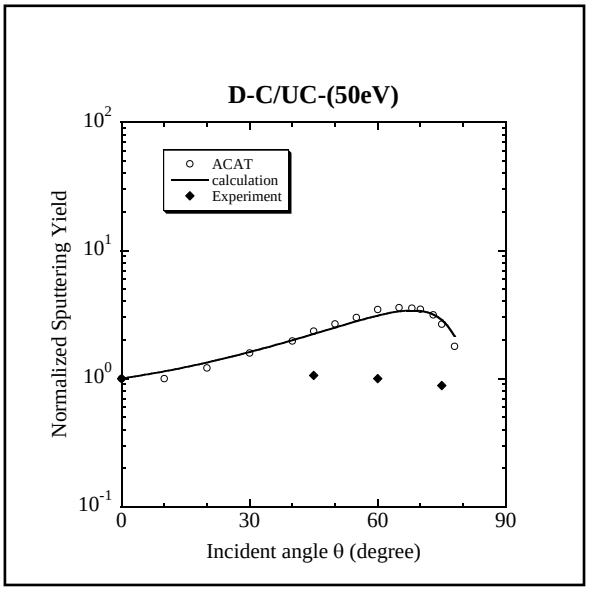

Fig. 22 Normalized sputtering yield vs. incident angle by the formula with the functions, the ACAT data, and the experimental data for C/UC- material irradiated by D^+ ions with 50eV.

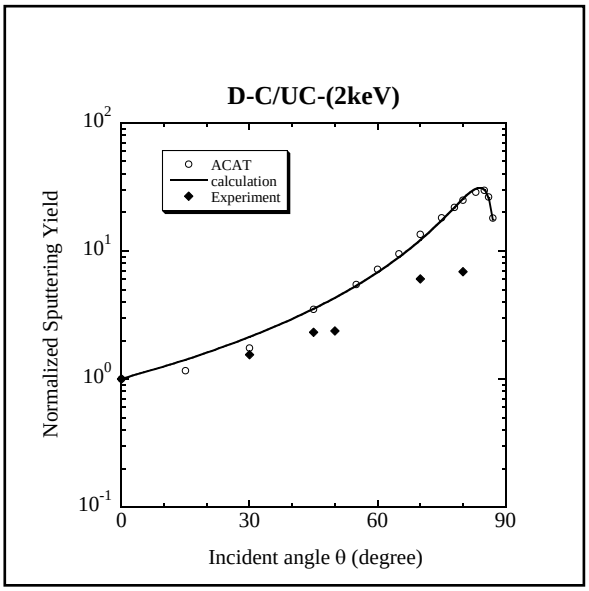

Fig. 23 Normalized sputtering yield vs. incident angle by the formula with the functions, the ACAT data, and the experimental data for C/UC- material irradiated by D^+ ions with 2keV.

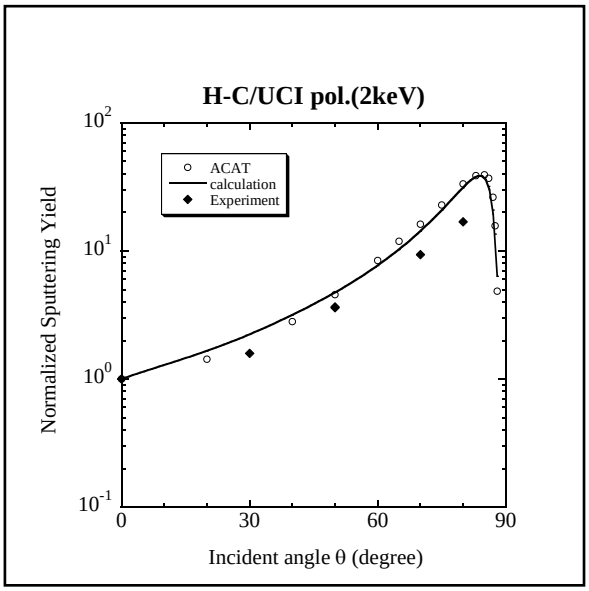

Fig. 24 Normalized sputtering yield vs. incident angle by the formula with the functions, the ACAT data, and the experimental data for C/UCI pol. material irradiated by H^+ ions with 2keV.

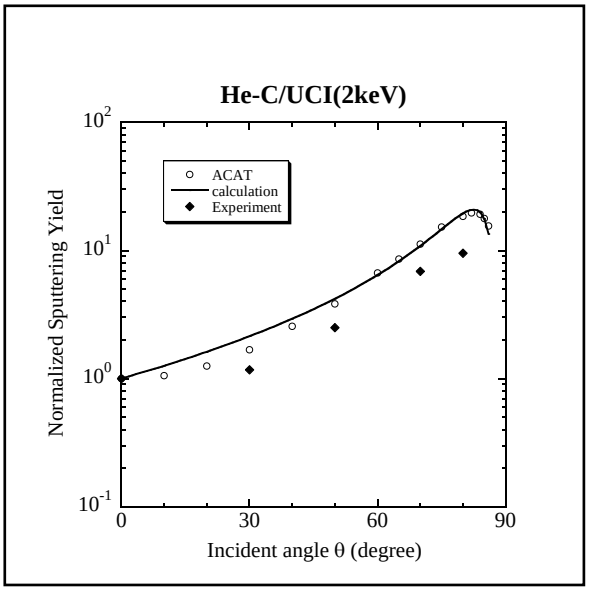

Fig. 25 Normalized sputtering yield vs. incident angle by the formula with the functions, the ACAT data, and the experimental data for C/UCI material irradiated by He^+ ions with 2keV.

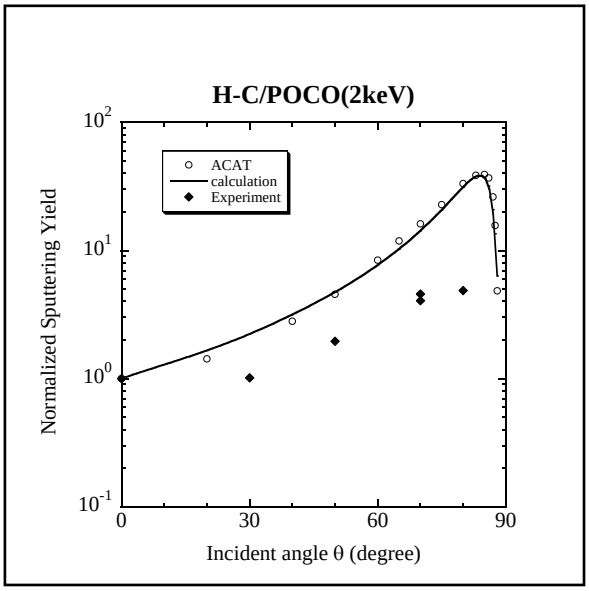

Fig. 26 Normalized sputtering yield vs. incident angle by the formula with the functions, the ACAT data, and the experimental data for C/POCO material irradiated by H^+ ions with 2keV.

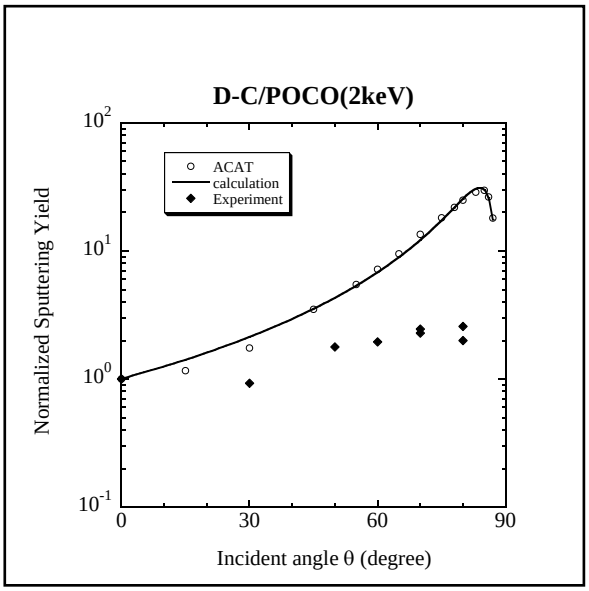

Fig. 27 Normalized sputtering yield vs. incident angle by the formula with the functions, the ACAT data, and the experimental data for C/POCO material irradiated by D^+ ions with 2keV.

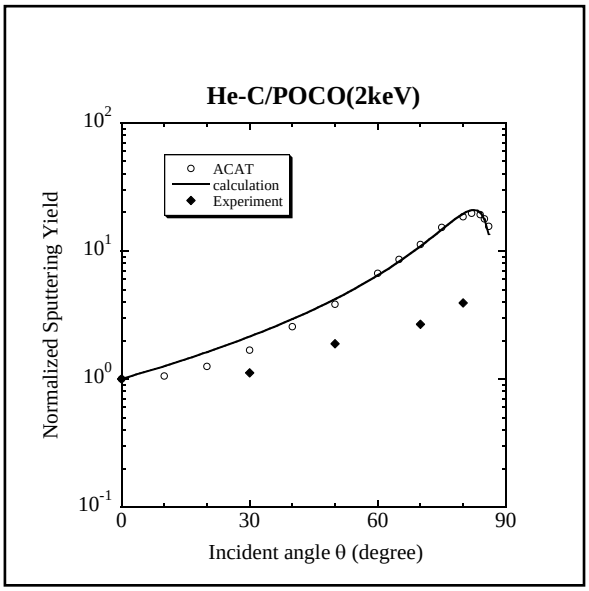

Fig. 28 Normalized sputtering yield vs. incident angle by the formula with the functions, the ACAT data, and the experimental data for C/POCO material irradiated by He^+ ions with 2keV.

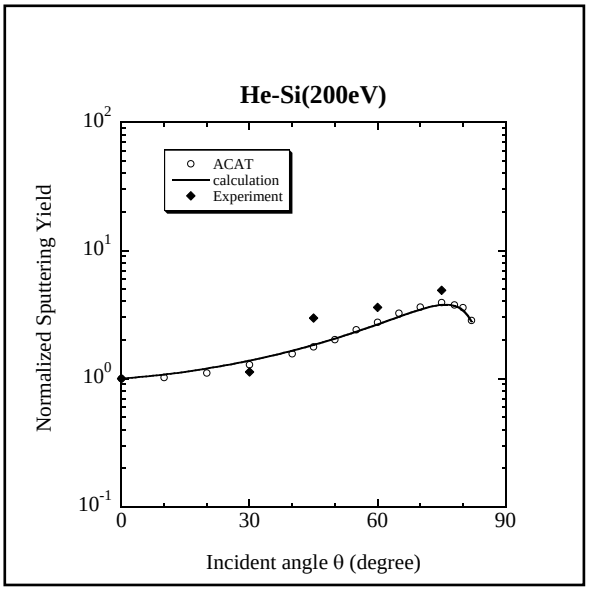

Fig. 29 Normalized sputtering yield vs. incident angle by the formula with the functions, the ACAT data, and the experimental data for Si material irradiated by He^+ ions with 200eV.

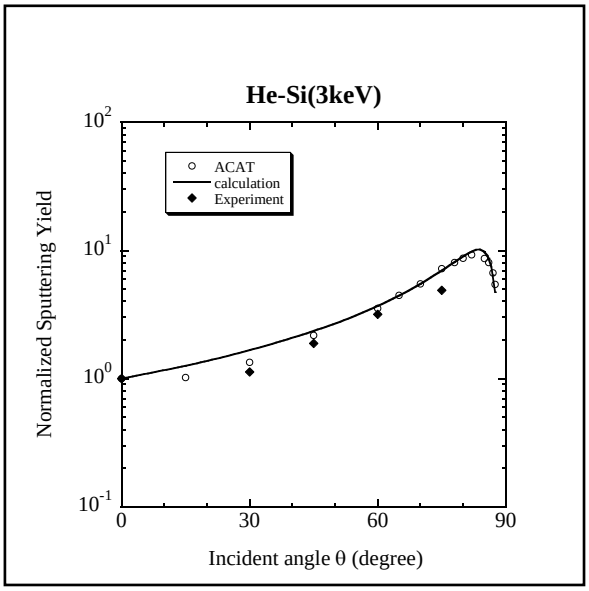

Fig. 30 Normalized sputtering yield vs. incident angle by the formula with the functions, the ACAT data, and the experimental data for Si material irradiated by He^+ ions with 3keV.

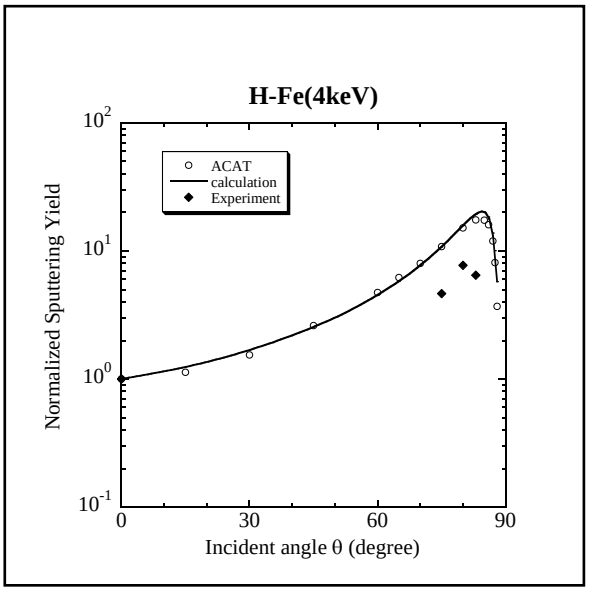

Fig. 31 Normalized sputtering yield vs. incident angle by the formula with the functions, the ACAT data, and the experimental data for Fe material irradiated by H^+ ions with 4keV.

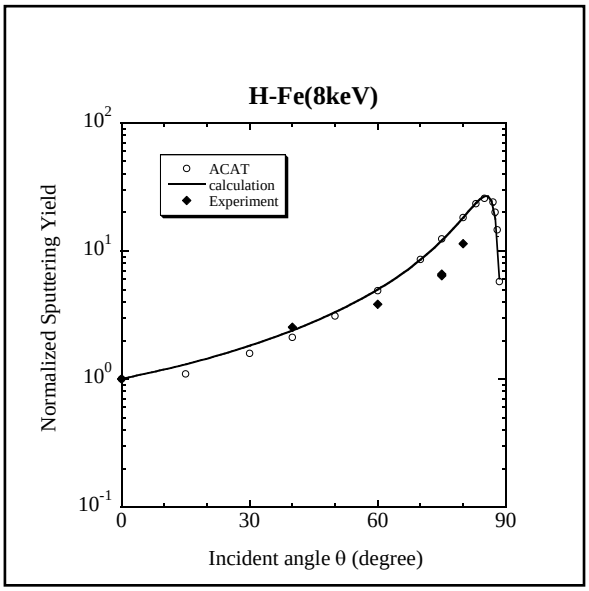

Fig. 32 Normalized sputtering yield vs. incident angle by the formula with the functions, the ACAT data, and the experimental data for Fe material irradiated by H^+ ions with 8keV.

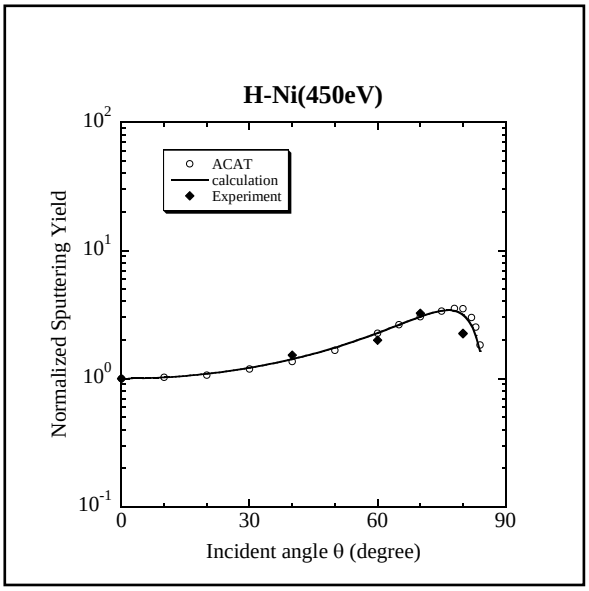

Fig. 33 Normalized sputtering yield vs. incident angle by the formula with the functions, the ACAT data, and the experimental data for Ni material irradiated by H^+ ions with 450eV.

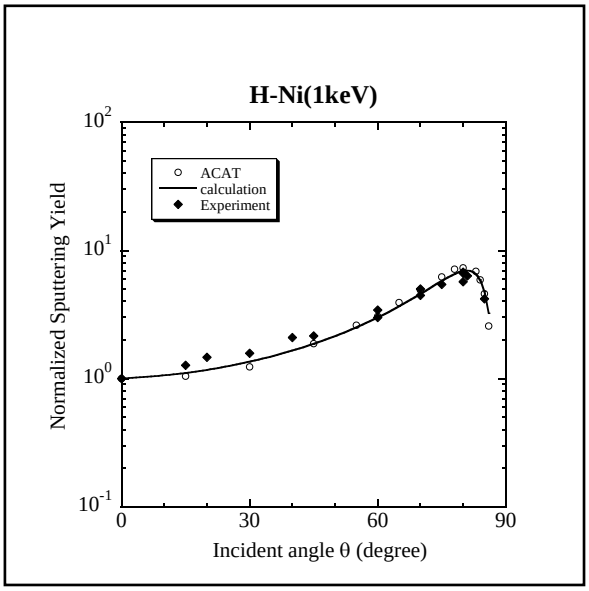

Fig. 34 Normalized sputtering yield vs. incident angle by the formula with the functions, the ACAT data, and the experimental data for Ni material irradiated by H^+ ions with 1keV.

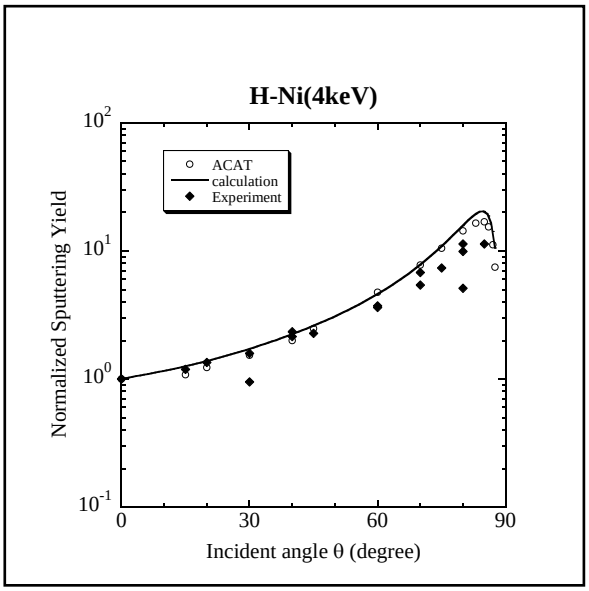

Fig. 35 Normalized sputtering yield vs. incident angle by the formula with the functions, the ACAT data, and the experimental data for Ni material irradiated by H^+ ions with 4keV.

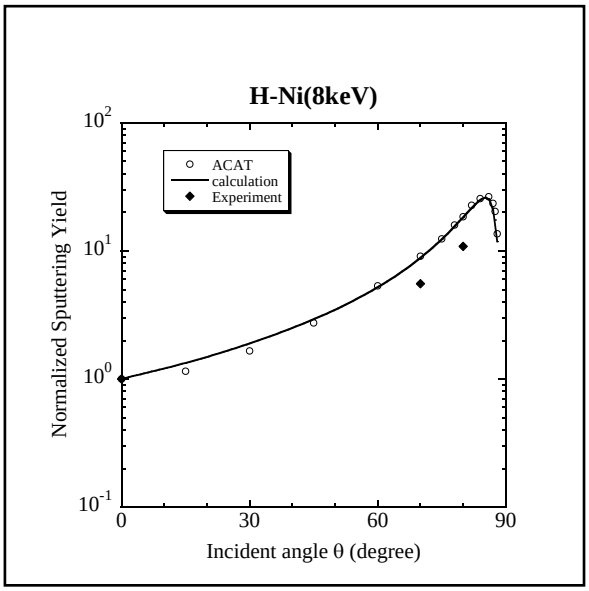

Fig. 36 Normalized sputtering yield vs. incident angle by the formula with the functions, the ACAT data, and the experimental data for Ni material irradiated by H^+ ions with 8keV.

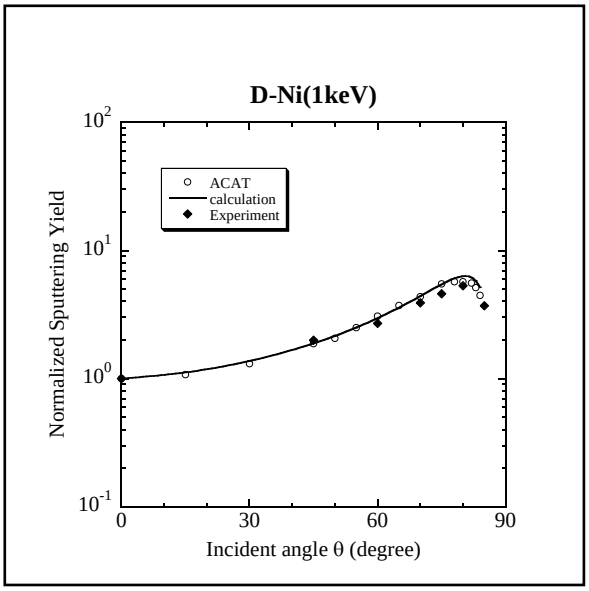

Fig. 37 Normalized sputtering yield vs. incident angle by the formula with the functions, the ACAT data, and the experimental data for Ni material irradiated by D^+ ions with 1keV.

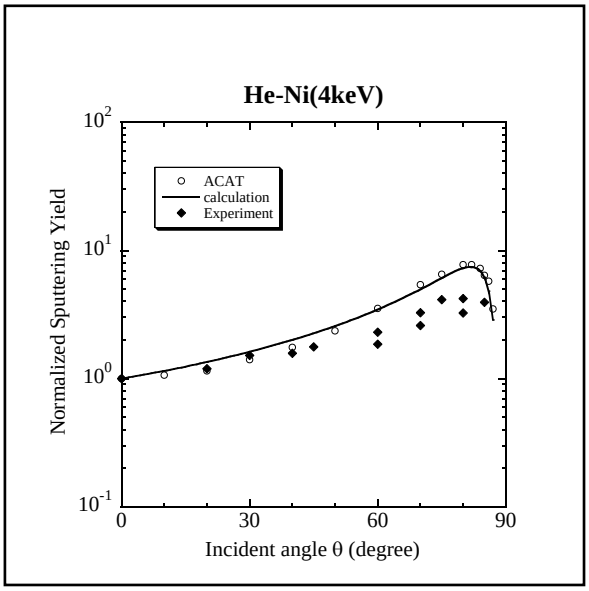

Fig. 38 Normalized sputtering yield vs. incident angle by the formula with the functions, the ACAT data, and the experimental data for Ni material irradiated by He^+ ions with 4keV.

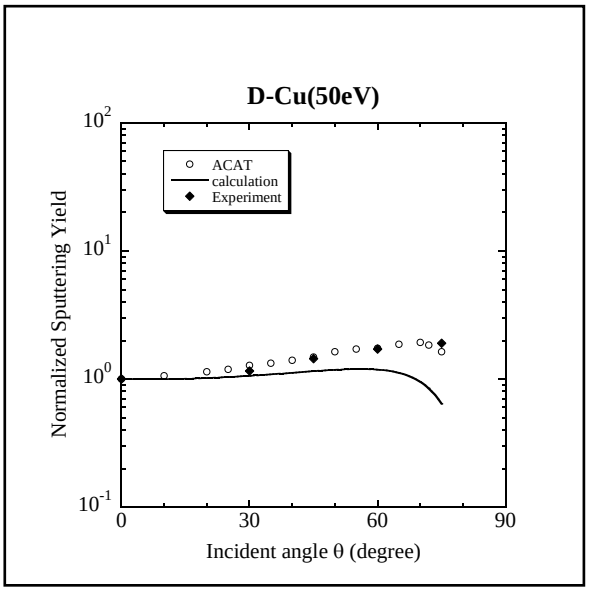

Fig. 39 Normalized sputtering yield vs. incident angle by the formula with the functions, the ACAT data, and the experimental data for Cu material irradiated by D^+ ions with 50eV.

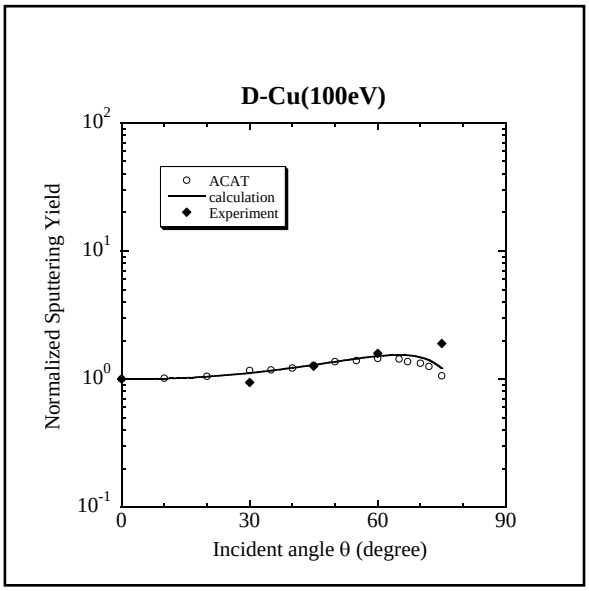

Fig. 40 Normalized sputtering yield vs. incident angle by the formula with the functions, the ACAT data, and the experimental data for Cu material irradiated by D^+ ions with 100eV.

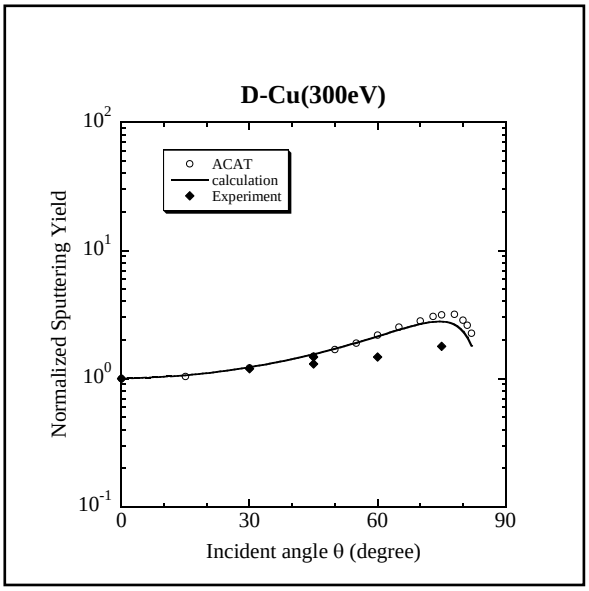

Fig. 41 Normalized sputtering yield vs. incident angle by the formula with the functions, the ACAT data, and the experimental data for Cu material irradiated by D^+ ions with 300eV.

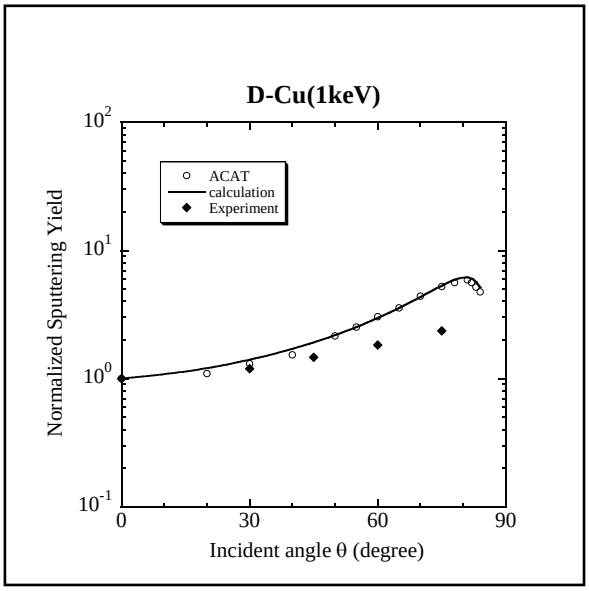

Fig. 42 Normalized sputtering yield vs. incident angle by the formula with the functions, the ACAT data, and the experimental data for Cu material irradiated by D^+ ions with 1keV.

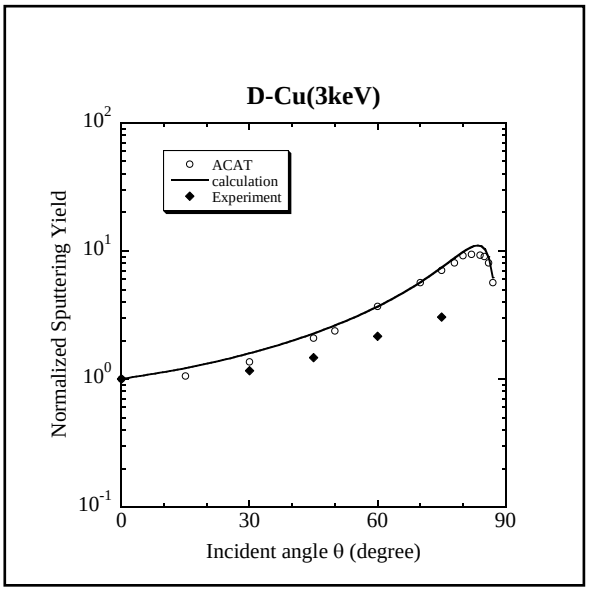

Fig. 43 Normalized sputtering yield vs. incident angle by the formula with the functions, the ACAT data, and the experimental data for Cu material irradiated by D^+ ions with 3keV.

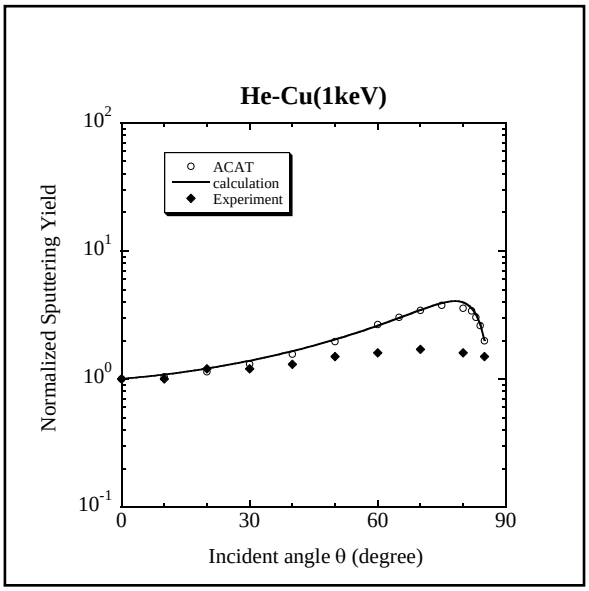

Fig. 44 Normalized sputtering yield vs. incident angle by the formula with the functions, the ACAT data, and the experimental data for Cu material irradiated by He^+ ions with 1keV.

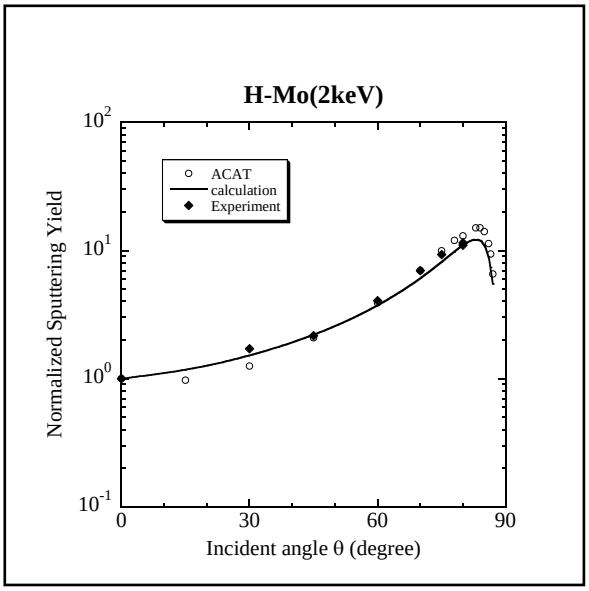

Fig. 45 Normalized sputtering yield vs. incident angle by the formula with the functions, the ACAT data, and the experimental data for Mo material irradiated by H^+ ions with 2keV.

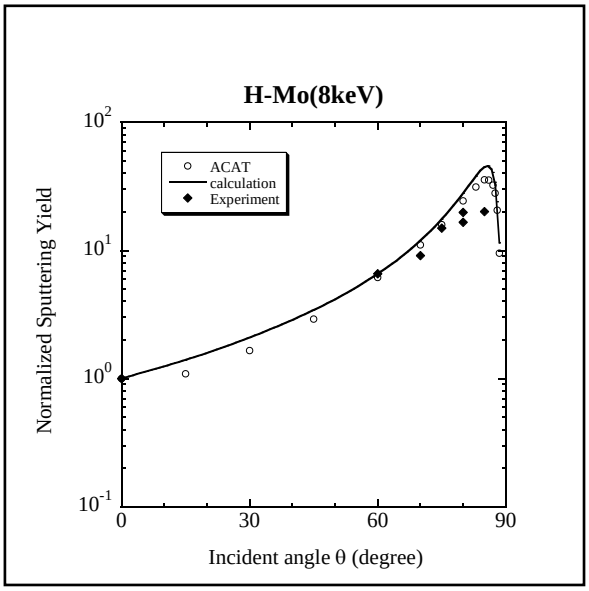

Fig. 46 Normalized sputtering yield vs. incident angle by the formula with the functions, the ACAT data, and the experimental data for Mo material irradiated by H^+ ions with 8keV.

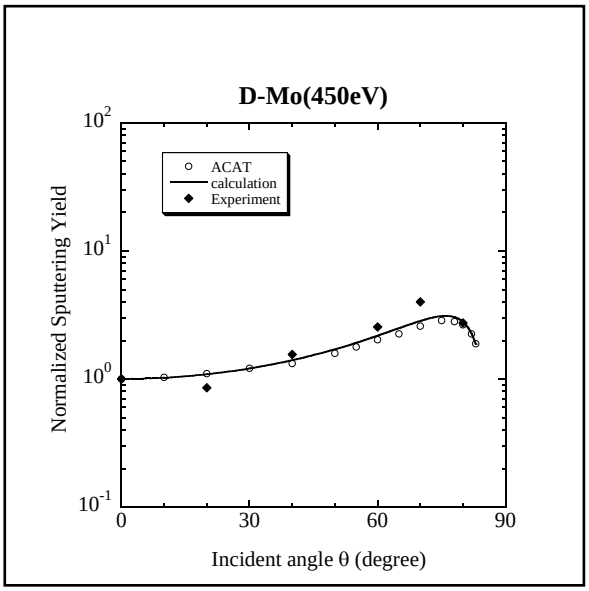

Fig. 47 Normalized sputtering yield vs. incident angle by the formula with the functions, the ACAT data, and the experimental data for Mo material irradiated by D^+ ions with 450eV.

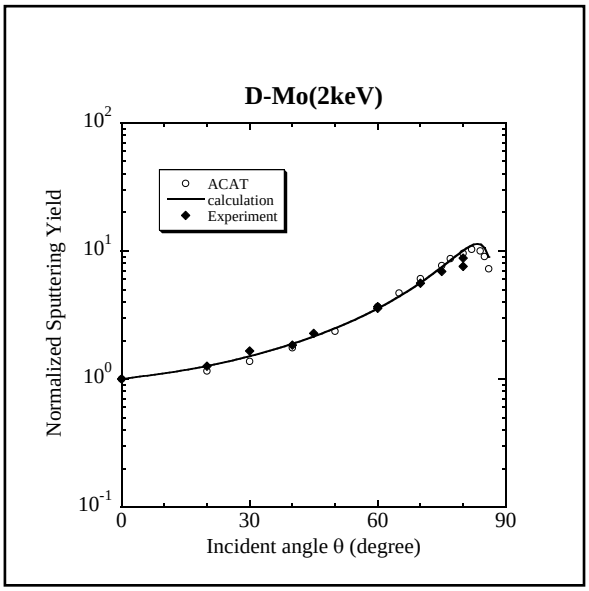

Fig. 48 Normalized sputtering yield vs. incident angle by the formula with the functions, the ACAT data, and the experimental data for Mo material irradiated by D^+ ions with 2keV.

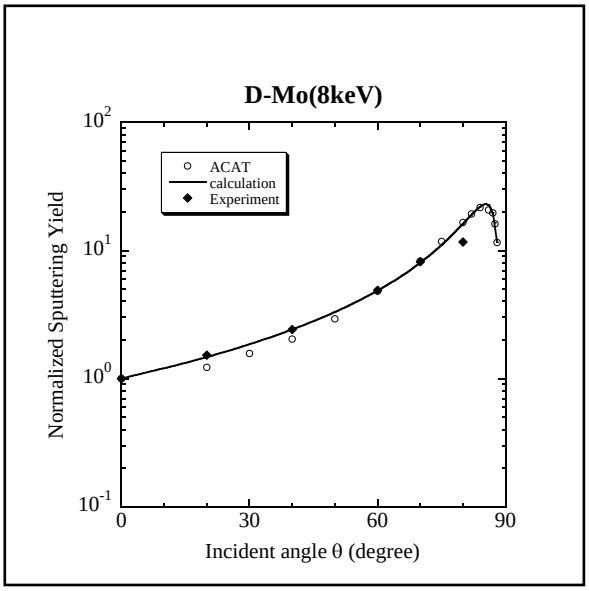

Fig. 49 Normalized sputtering yield vs. incident angle by the formula with the functions, the ACAT data, and the experimental data for Mo material irradiated by D^+ ions with 8keV.

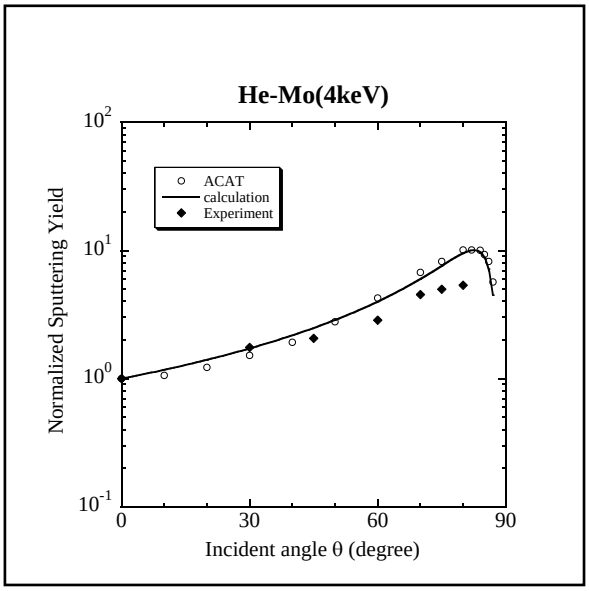

Fig. 50 Normalized sputtering yield vs. incident angle by the formula with the functions, the ACAT data, and the experimental data for Mo material irradiated by He^+ ions with 4keV.

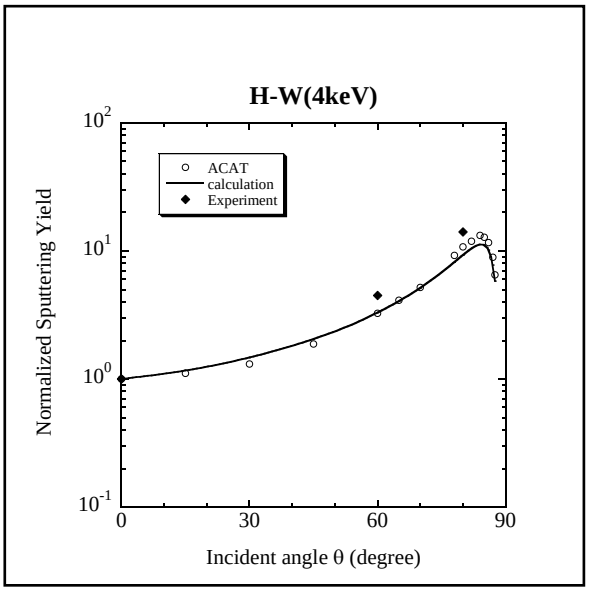

Fig. 51 Normalized sputtering yield vs. incident angle by the formula with the functions, the ACAT data, and the experimental data for W material irradiated by H^+ ions with 4keV.